ON THE SYNTHESIS OF THE VERTICAL PLANE PATTERNS OF ATCRBS ANTENNAS

Dipak L. Sengupta

ABSTRACT

Synthesis of the vertical plane patterns of ATCRBS antennas by linear arrays of isotropic elements are discussed. The synthesis method discussed here is based on the Fourier techniques which approximate the desired pattern in the least mean square sense. Analytical expressions have been derived for the field gradient obtainable from an antenna of given aperture length. The results have been applied to study the pattern characteristics of various improved ATCRBS antennas. The theoretical results compare fairly well with the measured values. It is recommended that further work be done on this problem to maximize the field gradient of an antenna of given length.

key words:

aperture synthesis

field gradient of antennas

sector beam patterns

improved ATCRBS antennas

MISSING
PAGE

PREFACE

This report investigates theoretically the field gradient (or the elevation plane pattern roll-off) at the boundaries of the pattern beams produced by linear aperture antennas designed on the basis of Fourier synthesis techniques. Both continuous aperture antenna and linear arrays of odd and even number of discrete isotropic elements are considered. Analytical expressions are derived for the field gradients in $dB/1^{o}$ as functions of the various antenna parameters. Theoretical results compare favorably with the corresponding measured values for the improved ATCRBS antennas.

MISSING
PAGE

TABLE OF CONTENTS

LIST OF ILLUSTRATIONS

LIST OF TABLES

1. INTRODUCTION

It is known [1, 2] that the undesirable effects of ground reflection and of certain multipath sources located on or near ground on the ATCRBS performance are considerably reduced if the free space vertical (or elevation) plane patterns of the beacon antennas possess large field gradients or the elevation pattern roll-offs at the horizon. The field gradient at the horizon for an antenna is defined to be the rate of decay of the free space far field in the elevation plane just below the horizon. It is usually expressed in dB per degree. Sometimes it is found convenient to define the field gradient in a direction which corresponds to a point 6 dB below the maximum value of the elevation plane beam. When the 6-dB point of the beam is directed along the horizon, the two definitions give identical values for the field gradient. The existing ATCRBS antenna uses a 2-foot (about 2λ) vertical aperture and its measured field gradient at the 6-dB point has been found to be 0.37 dB/1^{o}. By using longer vertical apertures, various improved ATCRBS antennas have been designed to have larger field gradients [3 - 5]. For example, the 4'-aperture Hazeltine open array and 8'-aperture Westinghouse array antennas have measured field gradients of 1.14 dB/1^{o} and 2.5 dB/1^{o} respectively.

From physical considerations it is expected that the field gradient of an antenna should increase with an increase of its vertical aperture. In the present report we develop some principles which will provide some guidelines to estimate quantitatively the amount of field gradient that may be obtained from a given vertical aperture. The ultimate objective of the present investigation is to estimate the largest field gradient compatible with a large value of the field at the horizon that can be achieved from an antenna with a given vertical aperture. Of course, the elevation plane pattern of the antenna must also satisfy the other desired requirements with respect to sidelobe level, beamwidth, etc.

The proper way to study such a problem would be to formulate it as an aperture synthesis problem with appropriate constraints on the desired pattern. However, in this study we follow a simpler approach based on Fourier synthesis techniques so that some approximate design principles may be developed without sophisticated analysis. Another reason for the approach followed here is that the

elevation patterns of most of the improved ATCRBS antennas have been designed by Fourier techniques.

The outline of the report is as follows. Section 2 considers the synthesis of a continuous linear source distribution and the field gradients obtained thereof. It is found that the continuous aperture results give a good rough indication of the field gradients that are obtained in practice. Section 3 discusses the synthesis of the elevation plane pattern using a linear aperture of discrete elements. Theoretical expressions are derived for the field gradients obtainable from such antennas designed by Fourier techniques. Section 4 gives a general discussion.

2. CONTINUOUS LINEAR APERTURE

Consider an aperture of length L aligned along the vertical x-axis as shown in Fig. 1. The angles in space are measured from the normal to the aperture so that

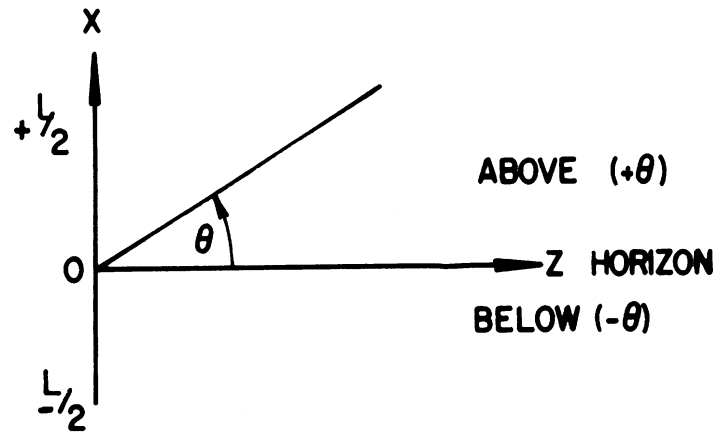

FIG. 1: A continuous aperture of length L.

the horizon is in the direction $\theta = 0^{o}$. Plotted as a function $u = \sin\theta$, the ideal free space elevation plane pattern function of the antenna is of sector beam shape and may be represented by

$$F_i(u) = 1, \qquad 0 \leq u \leq u_1 = \sin\theta_1$$
$$= 0 \qquad \text{otherwise.} \tag{1}$$

Note that in the visible region of space the range of u is $-1 \leq u \leq +1$. Fig. 2 shows a sketch of the ideal sector beam pattern for which the source distribution is to be

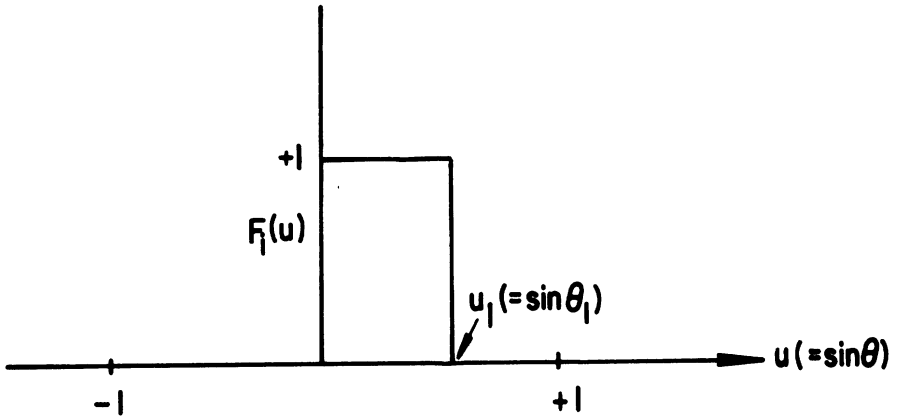

FIG. 2: The ideal pattern of the antenna.

synthesized. The parameter u_1 shown in Fig. 2 is governed by the desired coverage and the beamwidth of the antenna.

The source distribution f(x) necessary to synthesize the pattern given in Fig. 2 may be obtained by using the following Fourier transform relations [6]:

$$F_i(ku) = \int_{-\infty}^{\infty} f(x)\exp(ikux)dx \ , \tag{2}$$

$$f(x) = \frac{1}{2\pi} \int_{-\infty}^{\infty} F_i(ku)\exp(-ikux)d(ku) \ , \tag{3}$$

where $k = 2\pi/\lambda$ is the free space propagation constant. Since for all practical antennas the aperture lengths are finite, the pattern produced by the synthesized antenna will be given by

$$F_s(ku) = \int_{-L/2}^{L/2} f(x)\exp(ikux)dx \ . \tag{4}$$

The source distribution function for the present case may be obtained by using Eqs. (1) and (3) and is given by

$$f(x) = \frac{1}{2\pi}\exp(-iku_1 x/2)\frac{\sin(ku_1 x/2)}{x/2} \ , \quad -L/2 \leq x \leq L/2 \ . \tag{5}$$

The far field pattern of the synthesized antenna may now be obtained by using Eqs. (5) and (4) and is given by

$$\begin{aligned} F_s(\theta) &= F_s(ku) \\ &= \frac{1}{\pi}\left\{ \mathrm{Si}(\pi L \sin\theta/\lambda) + \mathrm{Si}\left[\frac{\pi L}{\lambda}(\sin\theta_1 - \sin\theta)\right]\right\} , \end{aligned} \tag{6}$$

where Si(x) is the sine integral defined by

$$\mathrm{Si}(x) = \int_0^x \frac{\sin v}{v}\, dv \quad . \tag{7}$$

Note that from Eq. (6),

$$F_s(0) = \frac{1}{\pi}\,\mathrm{Si}\left(\frac{\pi L}{\lambda}\sin\theta_1\right) = F_s(\theta_1) \quad , \tag{8}$$

which predicts that the field at the horizon will depend on the parameter θ_1.

The slope of the pattern in any direction θ in space may be obtained by differentiating Eq. (6) with respect to θ and is given by

$$F_s'(\theta) = \frac{L}{\lambda}\cos\theta\left\{\frac{\sin\left(\frac{\pi L}{\lambda}\sin\theta\right)}{\left(\frac{\pi L}{\lambda}\sin\theta\right)} - \frac{\sin\left[\frac{\pi L}{\lambda}(\sin\theta_1 - \sin\theta)\right]}{\left[\frac{\pi L}{\lambda}(\sin\theta_1 - \sin\theta)\right]}\right\} \tag{9}$$

Equation (9) indicates that the slope of the pattern at any point θ is proportional to the normalized aperture length L/λ. The slope at the horizon is from Eq. (9):

$$F_s'(0) = \frac{L}{\lambda}\left[1 - \frac{\sin\left(\frac{\pi L}{\lambda}\sin\theta_1\right)}{\left(\frac{\pi L}{\lambda}\sin\theta_1\right)}\right] \quad . \tag{10}$$

From Eq. (10) it may be concluded that for sufficiently large L/λ such that $\pi L/\lambda(\sin\theta_1) \gg 1$, the slope of the pattern is directly proportional to L/λ and is independent of the parameter θ_1. However, for small values of L/λ the slope may be increased beyond L/λ by proper choice of θ_1.

In order that the results may be applied directly to the measured patterns of an antenna, let us express the various results given above in terms of units used during measurement. It is normal practice to normalize a given antenna pattern with respect to the field at the beam maximum, i.e., normalized field in the direction of the beam maximum is unity. Expressed in dB the normalized elevation plane pattern of the antenna is given by

$$P(\theta) = 20\log_{10}\frac{F_s(\theta)}{F_m} \quad , \tag{11}$$

where F_m is the field in the direction of the maximum and $F_s(\theta)$ is as defined earlier and is a positive quantity. The field gradient $\alpha_g(\theta)$ in dB/1° at θ is now defined as

$$\alpha_g(\theta) = \frac{\pi}{180} P'(\theta) \quad . \tag{12}$$

Using Eqs. (11) and (12) it can be shown that

$$\alpha_g(\theta) = \frac{\pi}{180} \frac{20}{\log_e 10} \frac{F_s'(\theta)}{F_s(\theta)} \simeq 0.1518 \frac{F_s'(\theta)}{F_s(\theta)} \text{ dB/1}^\circ \quad . \tag{13}$$

Substituting Eqs. (6) and (9) in Eq. (13) we obtain the following:

$$\alpha_g(\theta) = 0.1518 \frac{L}{\lambda} \cos\theta \frac{\dfrac{\sin\left(\frac{\pi L \sin\theta}{\lambda}\right)}{\left(\frac{\pi L \sin\theta}{\lambda}\right)} - \dfrac{\sin\left[\frac{\pi L}{\lambda}(\sin\theta_1 - \sin\theta)\right]}{\left[\frac{\pi L}{\lambda}(\sin\theta_1 - \sin\theta)\right]}}{\frac{1}{\pi}\left\{\mathrm{Si}\left(\frac{\pi L \sin\theta}{\lambda}\right) + \mathrm{Si}\left[\frac{\pi L}{\lambda}(\sin\theta_1 - \sin\theta)\right]\right\}} \quad . \tag{14}$$

From Eq. (14) it follows that the field gradient at the horizon is given by

$$\alpha_g(0) = 0.1518(L/\lambda) \frac{1 - \dfrac{\sin\left(\frac{\pi L}{\lambda}\sin\theta_1\right)}{\left(\frac{\pi L}{\lambda}\sin\theta_1\right)}}{\frac{1}{\pi}\mathrm{Si}\left(\frac{\pi L}{\lambda}\sin\theta_1\right)} \quad . \tag{15}$$

Table 1 gives the field gradient values at the horizon, obtained from Eq. (15), as the quantity L/λ is varied and for values of $\theta_1 = \pi/6$ and $\pi/4$.

Table 1: Field Gradient in dB/1°

	$\alpha_g(0)$ in dB/1°	
L/λ	$\theta_1 = \pi/6$	$\theta_1 = \pi/4$
1	0.13	0.18
2	0.52	0.69
3	1.08	0.94
4	1.34	1.08
5	1.32	1.65
6	1.72	1.81
7	2.31	1.98
8	2.54	2.29
9	2.56	2.65
10	2.95	3.13
11	3.51	3.52

Figure 3 shows the variations of the field gradient with L/λ for $\theta_1 = \pi/6$ and $\pi/4$. For comparison the measured values of α_g for some ATCRBS antennas are also shown in Fig. 3. The results indicate that continuous aperture theory predicts fairly well the field gradients obtained from the improved ATCRBS antennas designed by Fourier techniques. The elevation plane patterns of ATCRBS antennas are usually obtained by linear arrays of discrete elements. It is therefore desirable to discuss the pattern synthesis and the field gradients of such antennas. This is done in the next section.

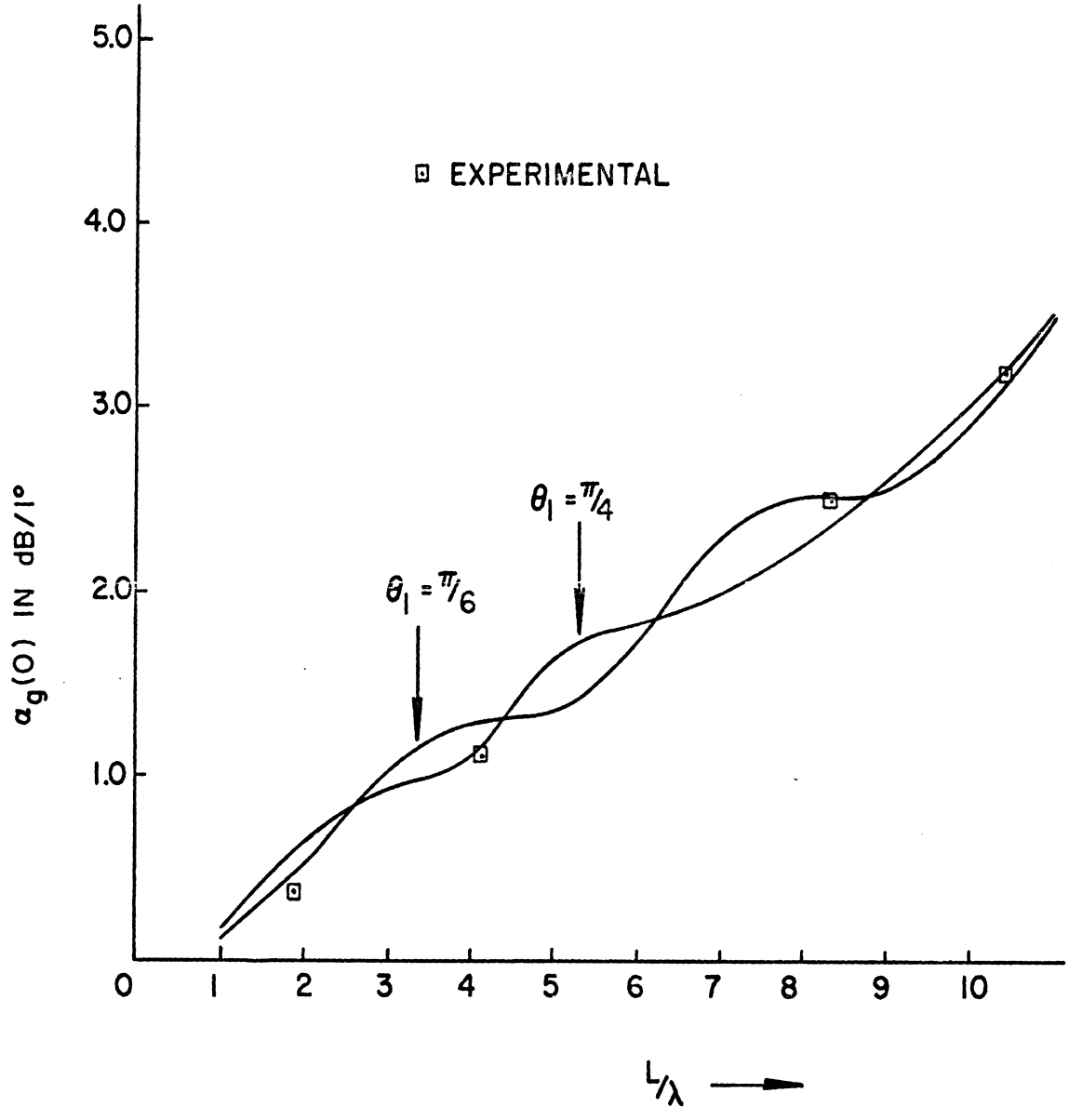

FIG. 3: Field gradient of a continuous aperture antenna as a function of L/λ for two values of θ_1.

3. LINEAR APERTURE OF DISCRETE ELEMENTS

The synthesis of a desired vertical plane pattern using a linear array of discrete elements is discussed in the present section. The cases of the linear aperture consisting of odd and even number of elements are discussed separately.

3.1 Linear Aperture of Odd Number of Elements

We assume that a linear aperture of length L is aligned along the x-axis which lies in the vertical direction. The linear aperture consists of an array of (2N+1) isotropic elements, uniformly spaced with interelement spacing d as shown in Fig. 4. Angles θ in space are measured from the normal to the aperture, so that $\theta = 0^{o}$ is the horizontal direction.

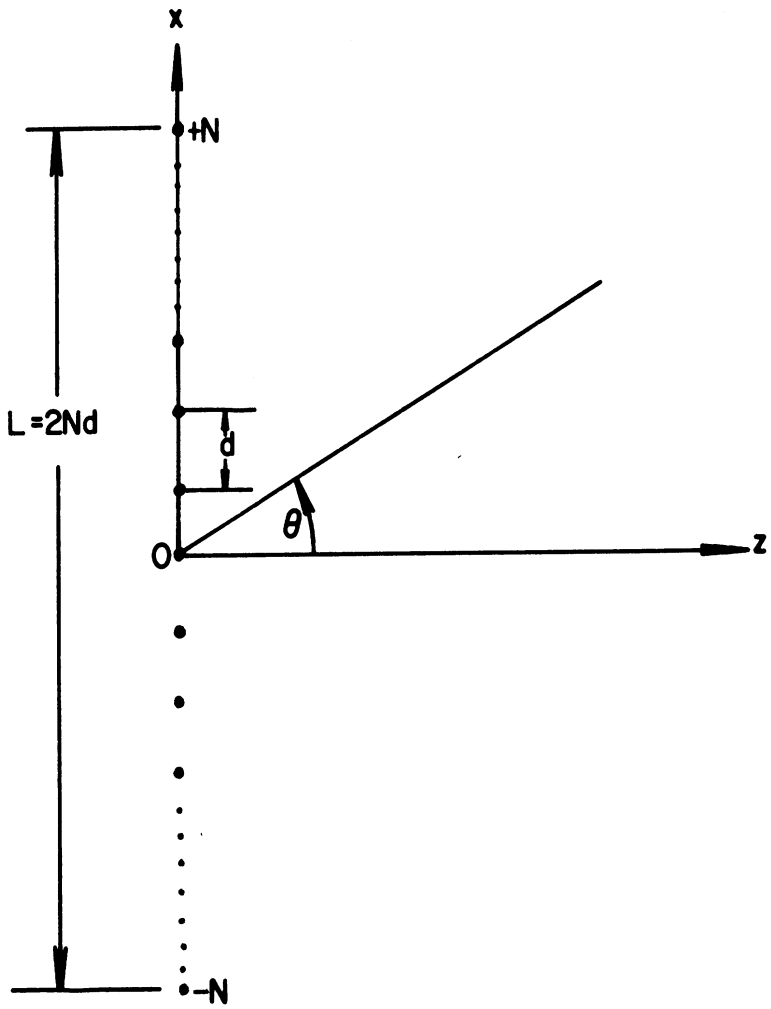

FIG. 4: Linear array of (2N+1) isotropic sources.

Plotted as a function of $u = \sin\theta$, the desired vertical plane pattern of the antenna is

$$\begin{aligned} F_i(u) &= 1 , && u_2(=\sin\theta_2) \leq u \leq u_1(=\sin\theta_1) \\ &= 0 , && \text{otherwise.} \end{aligned} \tag{16}$$

Figure 5 shows a sketch of the desired pattern given by Eq. 16. The parameters

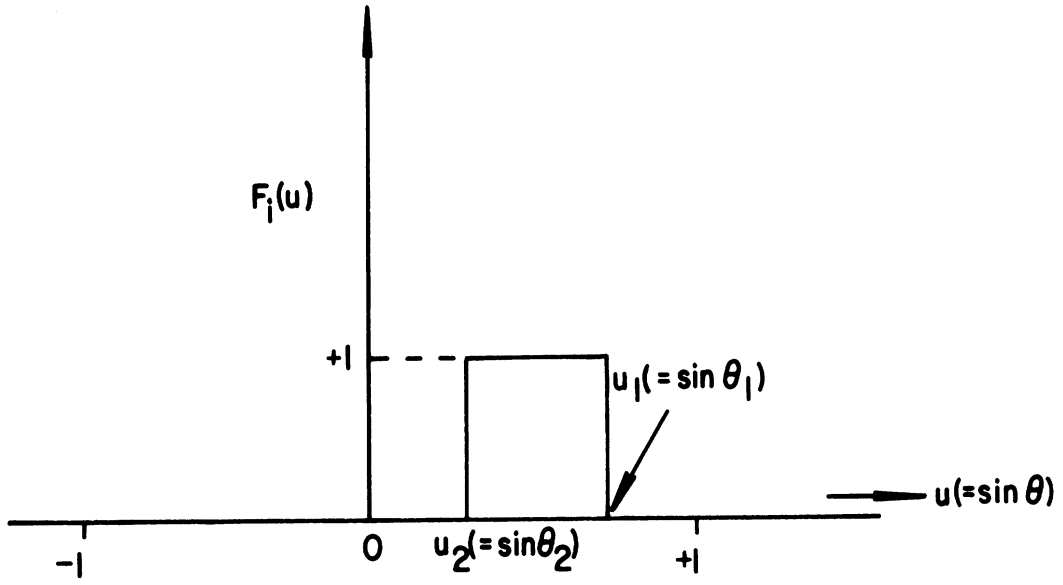

FIG. 5: Desired vertical plane pattern.

u_1 and u_2 are governed by the considerations of beamwidth, pattern slope, etc. We apply the Fourier synthesis techniques to obtain the required excitation of the source elements so that the synthesized pattern of the array approximates the desired pattern in the least mean square sense [6]. For this purpose it is natural to assume that the interelement spacing $d = \lambda/2$ which is also a convenient choice from practical considerations.

Let the excitation of the nth element be represented by $I_n e^{-i\alpha_n}$ where I_n is the amplitude and α_n is the phase of excitation. The far field pattern of an array of (2N+1) such elements, spaced $\lambda/2$ apart, is given by

$$F_s(\theta) = \sum_{-N}^{N} I_n e^{-i\alpha_n} e^{in\pi \sin\theta} . \tag{17}$$

By applying Fourier synthesis techniques, it can be shown [6] that to approximate the desired pattern given in Fig. 5, the array excitation coefficients I_n, α_n in Eq. (17) must be given by

$$I_n = \frac{\sin\left[\frac{n\pi}{2}(\sin\theta_1 - \sin\theta_2)\right]}{n\pi} , \tag{18}$$

$$\alpha_n = \frac{n\pi}{2}(\sin\theta_1 + \sin\theta_2) . \tag{19}$$

Note that the array excitation is such that $I_n = I_{-n}$ and $\alpha_n = -\alpha_{-n}$. After introducing Eqs. (18) and (19) into Eq. (17), the synthesized pattern may be written explicitly as follows:

$$F_s(\theta) = \frac{1}{2}(\sin\theta_1 - \sin\theta_2) + 2\sum_{1}^{N} \frac{\sin\left[\frac{n\pi}{2}(\sin\theta_1 - \sin\theta_2)\right]}{n\pi} \cos\left\{n\pi\left(\sin\theta - \frac{\sin\theta_1 + \sin\theta_2}{2}\right)\right\} \tag{20}$$

The slope of the pattern at any direction θ may be obtained by differentiating Eq. (20) with respect to θ and is given by

$$F_s'(\theta) = N\cos\theta \left\{ \cos\left[(N+1)\frac{\pi}{2}(\sin\theta - \sin\theta_2)\right] \frac{\sin\left[\frac{N\pi}{2}(\sin\theta - \sin\theta_2)\right]}{N\sin\left[\frac{\pi}{2}(\sin\theta - \sin\theta_1)\right]} - \cos\left[(N+1)\frac{\pi}{2}(\sin\theta - \sin\theta_1)\right] \frac{\sin\left[\frac{N\pi}{2}(\sin\theta - \sin\theta_1)\right]}{N\sin\left[\frac{\pi}{2}(\sin\theta - \sin\theta_1)\right]} \right\} \tag{21}$$

As in the continuous aperture case we assume that $\theta_2 = 0$. Under this condition the field and the pattern slope at the horizon are given by

$$F_s(0) = \frac{\sin\theta_1}{2} + \sum_{1}^{N} \frac{\sin(n\pi \sin\theta_1)}{n\pi} \quad , \tag{22}$$

$$F'_s(0) = N - \cos\left[(N+1)\frac{\pi}{2}\sin\theta_1\right] \frac{\sin\left(\frac{N\pi}{2}\sin\theta_1\right)}{\sin\left(\frac{\pi}{2}\sin\theta_1\right)} \quad . \tag{23}$$

The field gradient at any direction θ may be obtained by using Eqs. (13), (20) and (21). For the case with $\theta_2 = 0$, the field gradient at the horizon is given by

$$\alpha_g(0) = 0.1518 \frac{F'_s(0)}{F_s(0)}$$

$$= 0.1518 \frac{N - \cos\left[(N+1)\frac{\pi}{2}\sin\theta_1\right] \frac{\sin\left(\frac{N\pi}{2}\sin\theta_1\right)}{\sin\left(\frac{\pi}{2}\sin\theta_1\right)}}{\frac{\sin\theta_1}{2} + \sum_{1}^{N} \frac{\sin(n\pi\sin\theta_1)}{n\pi}} \quad . \tag{24}$$

Table 2 gives the field gradient in dB/1° at the horizon that can be obtained from a linear array of isotropic elements, spaced $\lambda/2$ apart, and containing (2N+1) elements. Note that the results are shown for two values of the parameter $\theta_1 = \pi/6$ and $\pi/4$. Observe that for $\lambda/2$-spacing between the elements the total aperture of the array is given by $L/\lambda = N$. The results shown in Table 1 indicate that for the range of N considered, the field gradient values are slightly different for the two values of θ.

Figure 6 shows $\alpha_g(0)$ vs. $N(= L/\lambda)$ for the linear array with odd number of elements. The corresponding measured values are also shown for comparison. It is found, in general, that the theoretical values seem to be larger than the measured values. For a given N, a judicious choice of θ_1 would yield the largest compatible value of α_g. Figure 7 shows $\alpha_g(0)$ vs. N(or L/λ) for the discrete and continuous aperture cases. The results for the linear array of discrete elements appear to be larger than those of the continuous array.

Table 2: Field gradient at the horizon $\alpha_g(0)$ in dB/1° for a linear array of (2N+1) elements.

$N = L/\lambda$	$\alpha_g(0)$ in dB/1°, $\theta_1 = \pi/6$	$\alpha_g(0)$ in dB/1°, $\theta_1 = \pi/4$
1	0.27	0.40
2	0.80	0.96
3	1.31	0.91
4	1.31	1.37
5	1.44	1.84
6	2.02	1.79
7	2.53	2.35
8	2.53	2.69
9	2.65	2.69
10	3.24	3.32

A typical pattern computed from Eq. (20) with N = 4, d = $\lambda/2$ (i.e., L = 4λ), $\theta_2 = 0^\circ$ and $\theta_1 = \pi/4$ is shown in Fig. 8. The field gradient at the horizon is found to be $\sim$1.37 dB. The sidelobe level is about 18dB. Note that the field gradient at $\theta = 0^\circ$ obtained from the continuous aperture theory for an aperture of length L = 4λ, $\theta_1 = \pi/4$ is about 1.08dB.

Equation (23) (or 24) indicates that for a given N, the parameter θ_1 may be chosen to obtain the largest slope of the pattern at $\theta = 0^\circ$. If θ_1 is chosen such that $\sin\theta_1 = (2M+1)/N$, M = 0, 1, 2... then it follows from Eq. (23) that

$$F_s'(0) = N+1, \quad \text{for} \quad \sin\theta_1 = \frac{2M+1}{N} \quad . \tag{25}$$

With N = 4, M = 1 we obtain from Eq. (25) $\theta_1 \simeq 51^\circ$. Figure 9 shows a pattern obtained for N = 4, d = $\lambda/2$, $\theta_2 = 0^\circ$ and $\theta_1 \simeq 51^\circ$. It can be seen from Fig. 9 that the field gradient in this case is about 1.5 dB which is slightly larger than that shown in Fig. 8. The sidelobe level in Fig. 9 is about 20 dB down.

Figures 10a - 10d show some selected patterns produced by linear arrays of odd number of elements designed according to $\theta_2 = 0^\circ$ and $\theta_1 = \pi/4$. From these patterns and also from Fig. 8 it appears that achieving 20 dB sidelobe is possible even with N = 4 (i.e., L = 4λ).

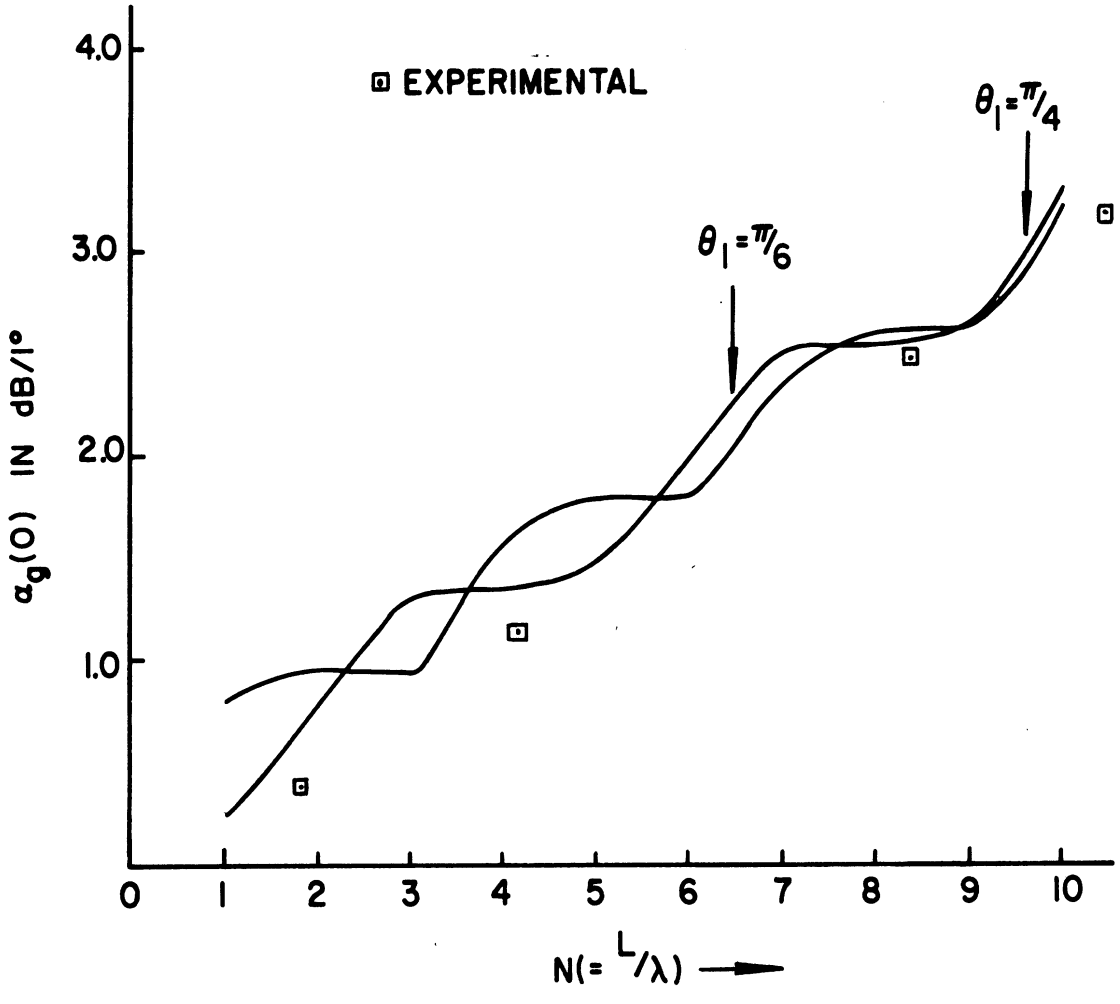

FIG. 6: Field gradient of a linear aperture of (2N+1) elements as a function of N (= L/λ) for two values of θ_1.

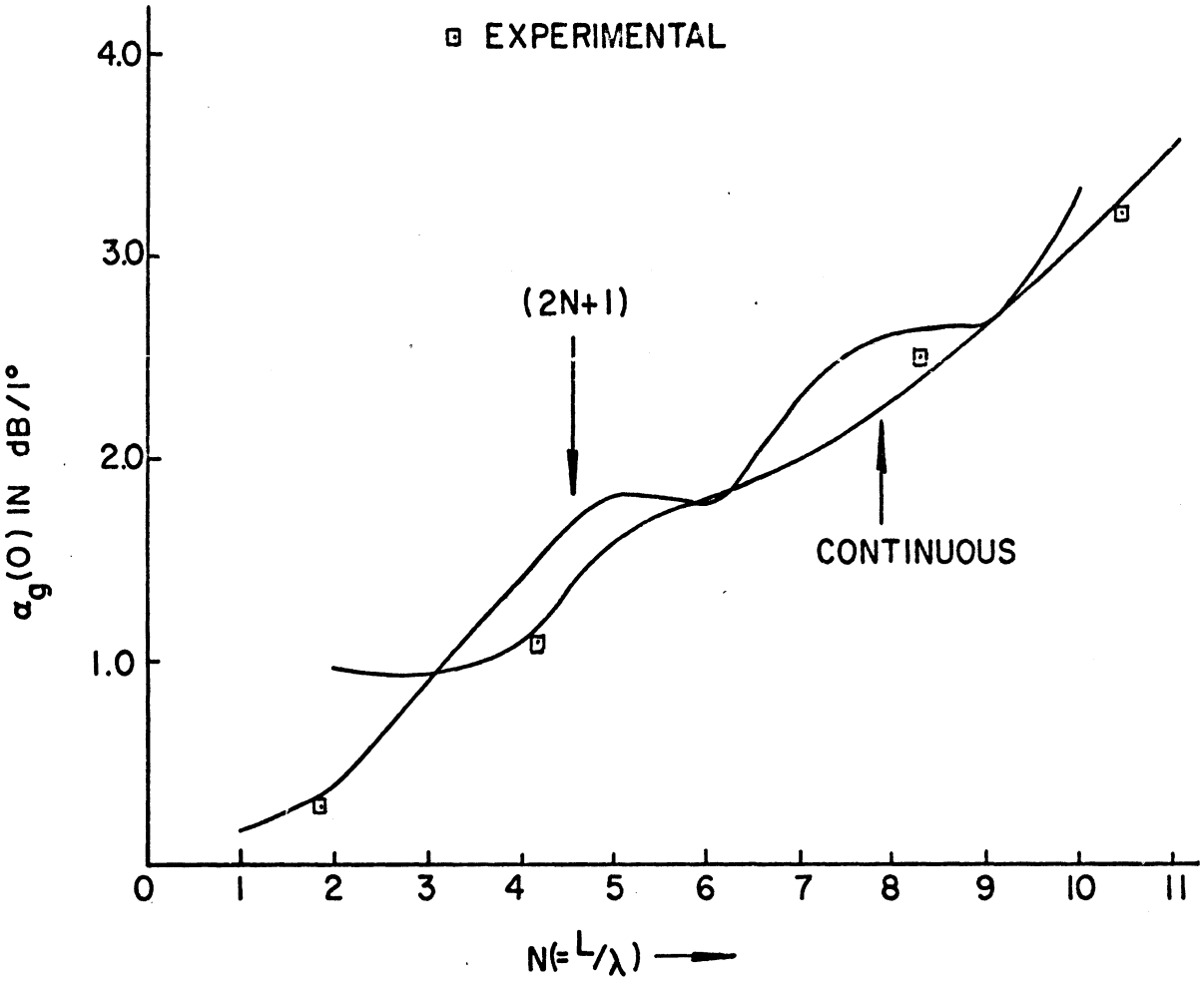

FIG. 7: Field gradients of continuous and discrete apertures as functions of length or number of elements, $\theta_1 = \pi/4$.

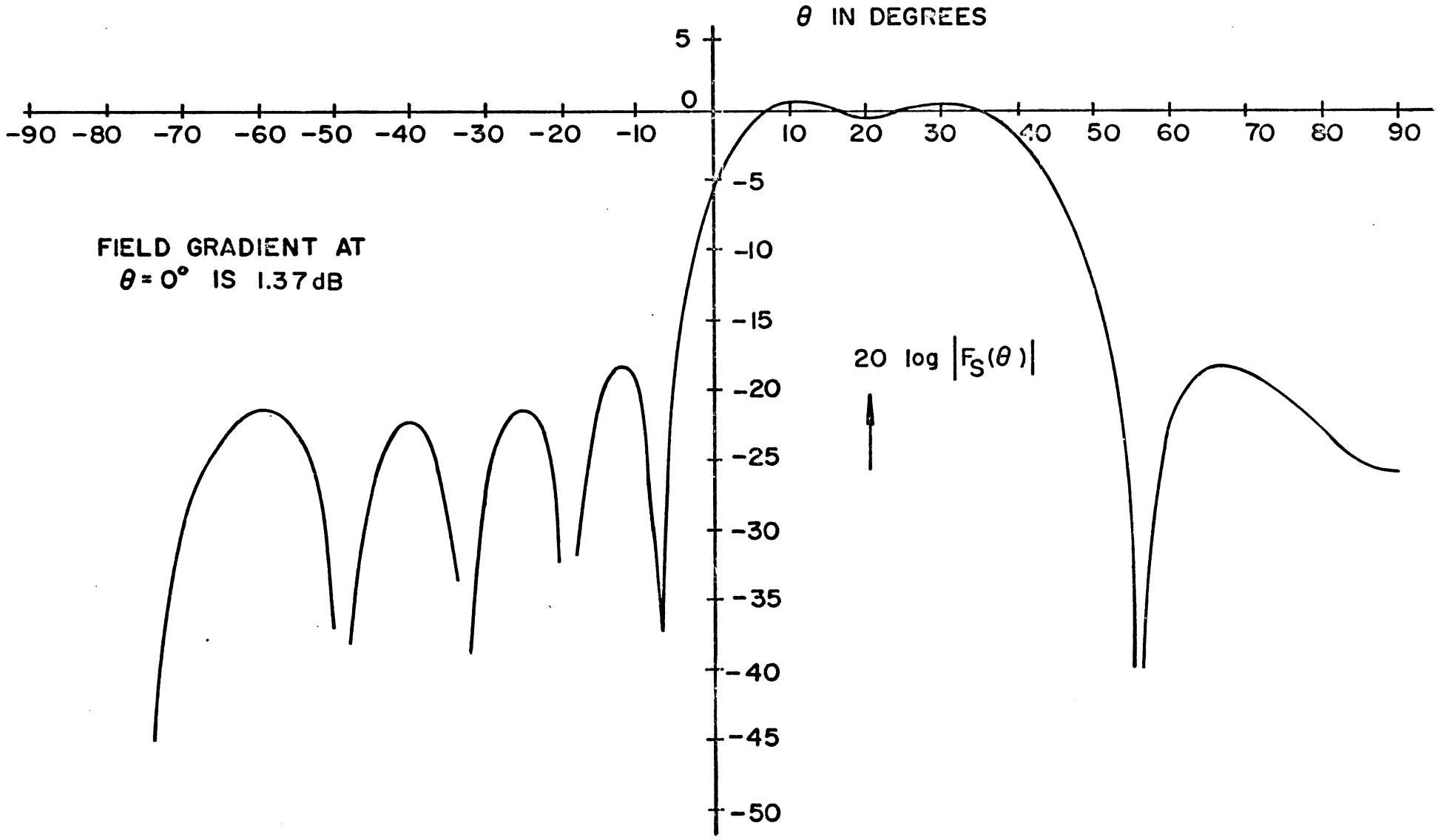

FIG. 8: Synthesized pattern for a linear array of (2N+1) elements. $L = 4\lambda$, $N = 4$, $d = \lambda/2$, $\theta_2 = 0^{\circ}$, $\theta_1 = \pi/4$.

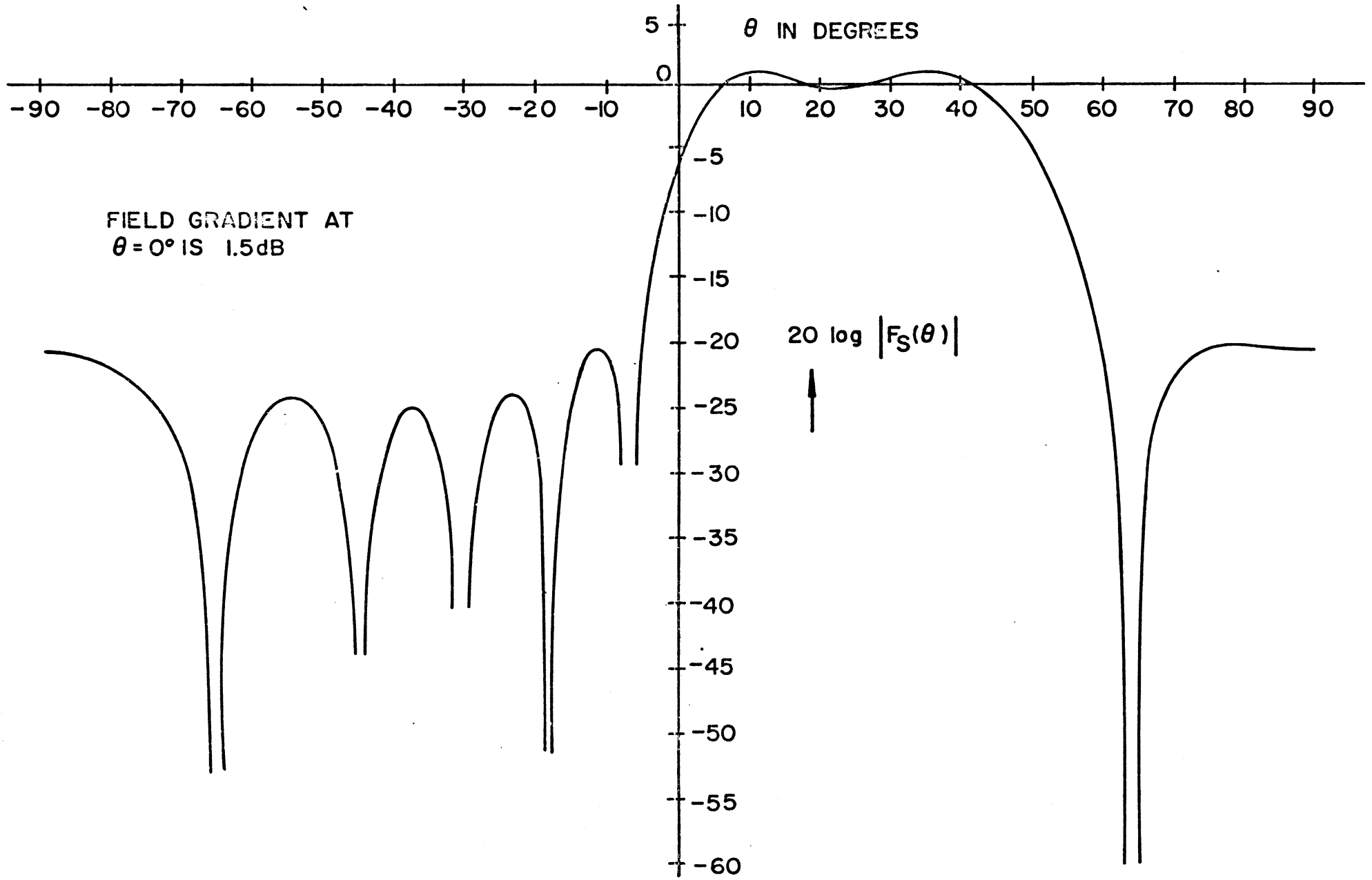

FIG. 9: Synthesized pattern for a linear array of (2N+1) elements, $L = 4\lambda$, $N = 4$, $d = \lambda/2$, $\theta_2 = 0^{\circ}$, $\theta_1 = 51^{\circ}$.

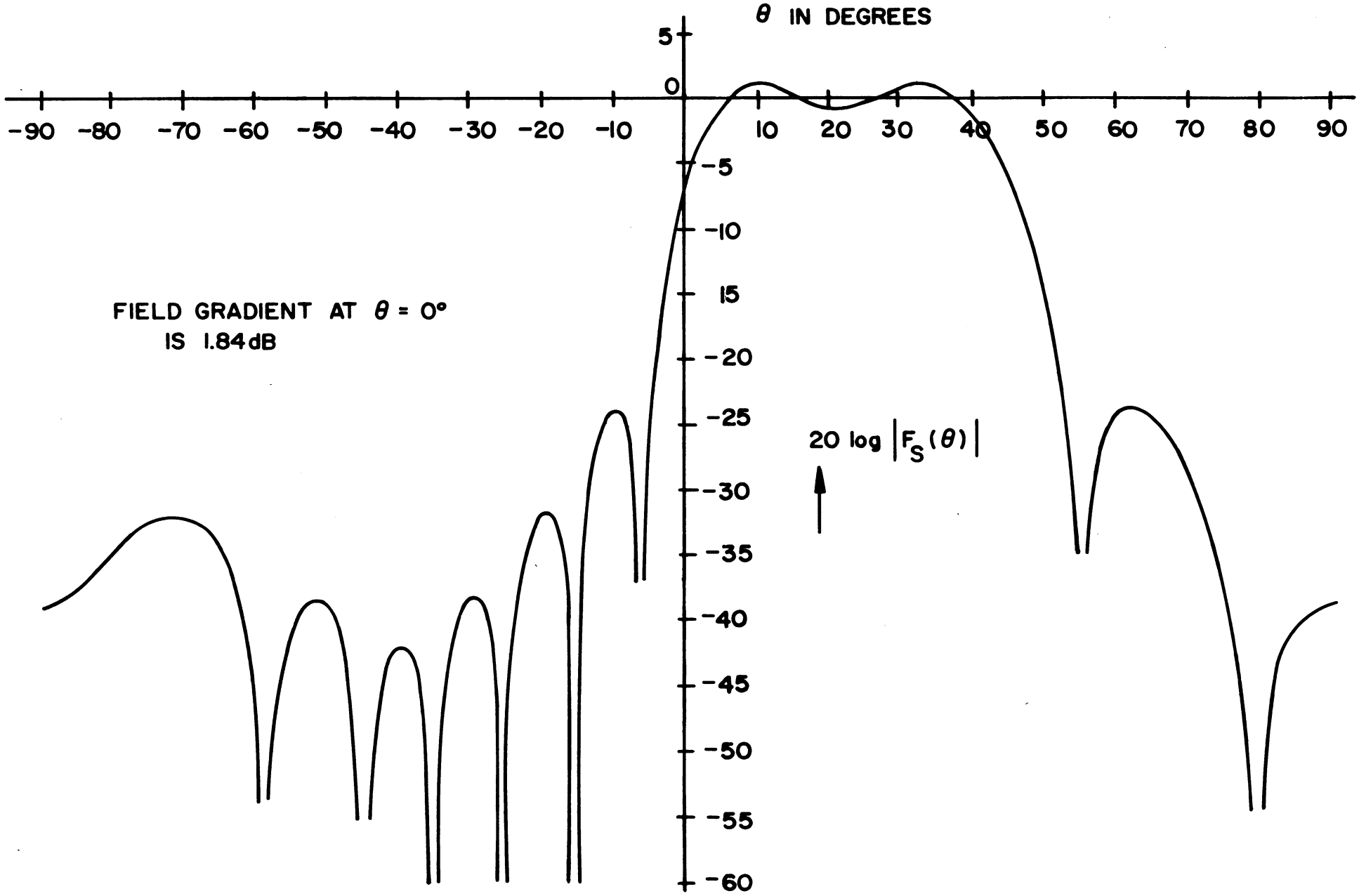

FIG. 10(a): Synthesized pattern for a linear array of (2N+1) elements, $L = 5\lambda$, $N = 5$, $d = \lambda/2$, $\theta_2 = 0^0$, $\theta_1 = \pi/4$.

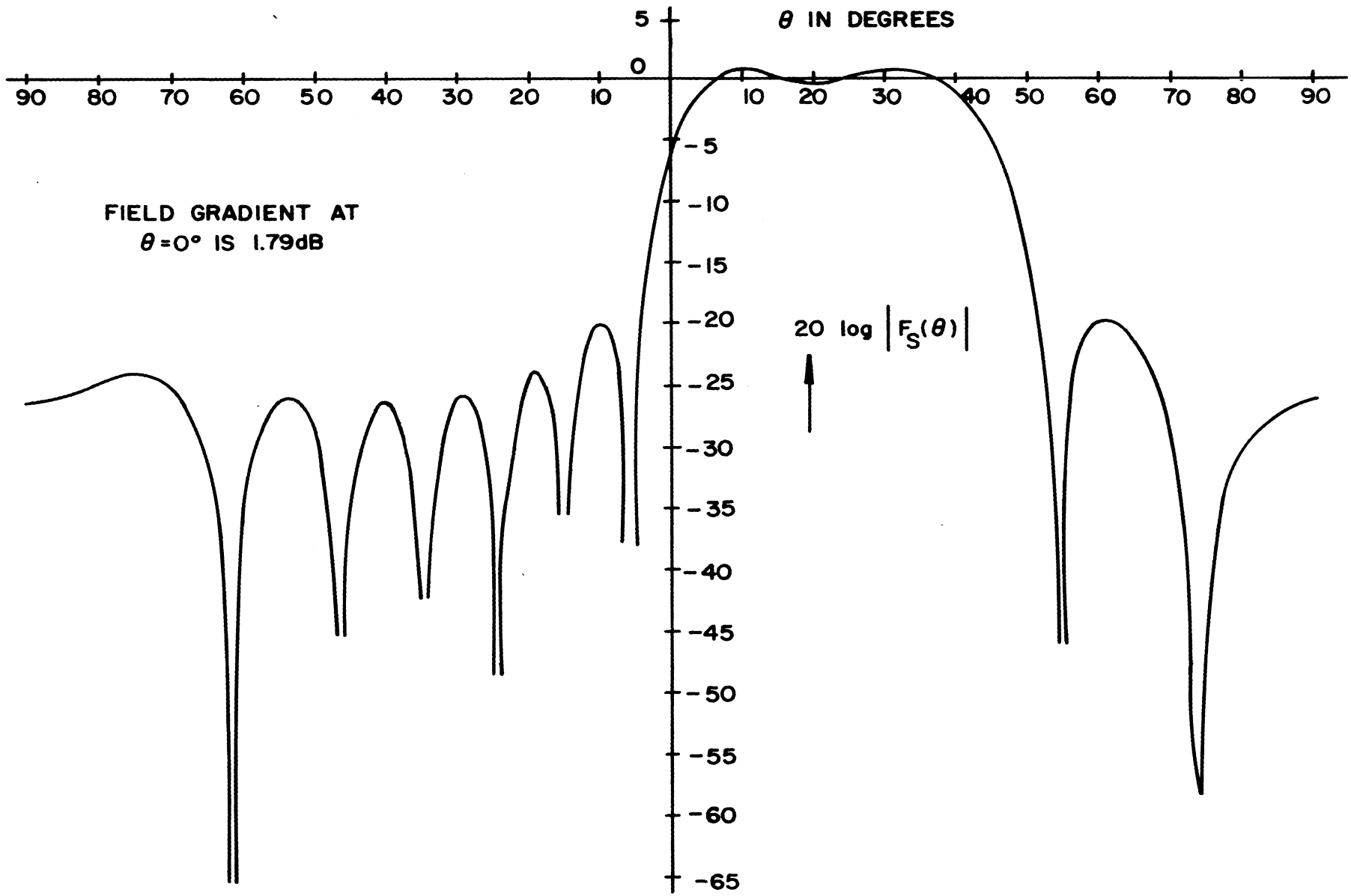

FIG. 10(b): Synthesized pattern for a linear array of (2N+1) elements. $L = 6\lambda$, $N = 6$, $d = \lambda/2$, $\theta_2 = 0^0$, $\theta_1 = \pi/4$.

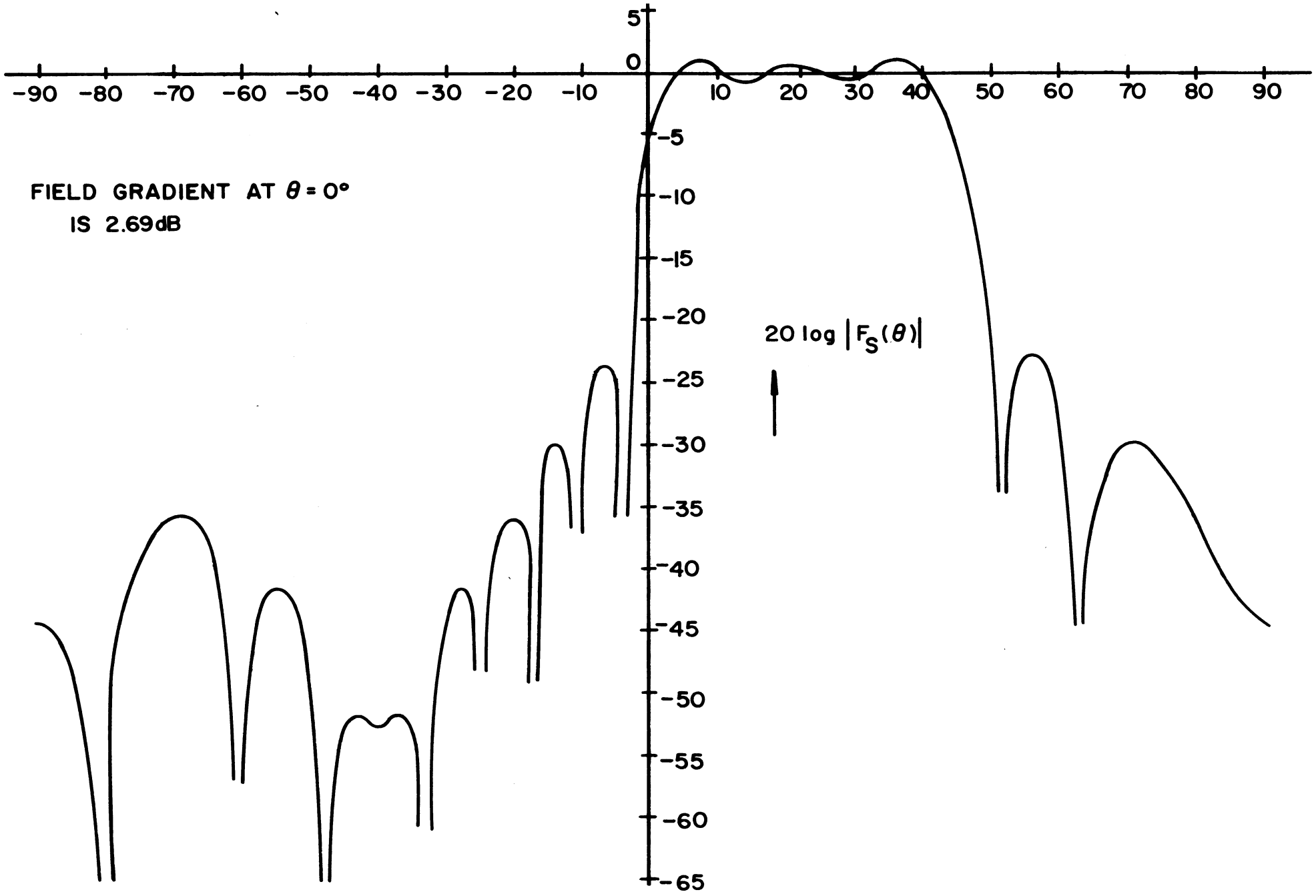

FIG. 10(c): Synthesized pattern for a linear array of (2N+1) elements. $L = 8\lambda$, $N = 8$, $d = \lambda/2$, $\theta_2 = 0^\circ$, $\theta_1 = \pi/4$.

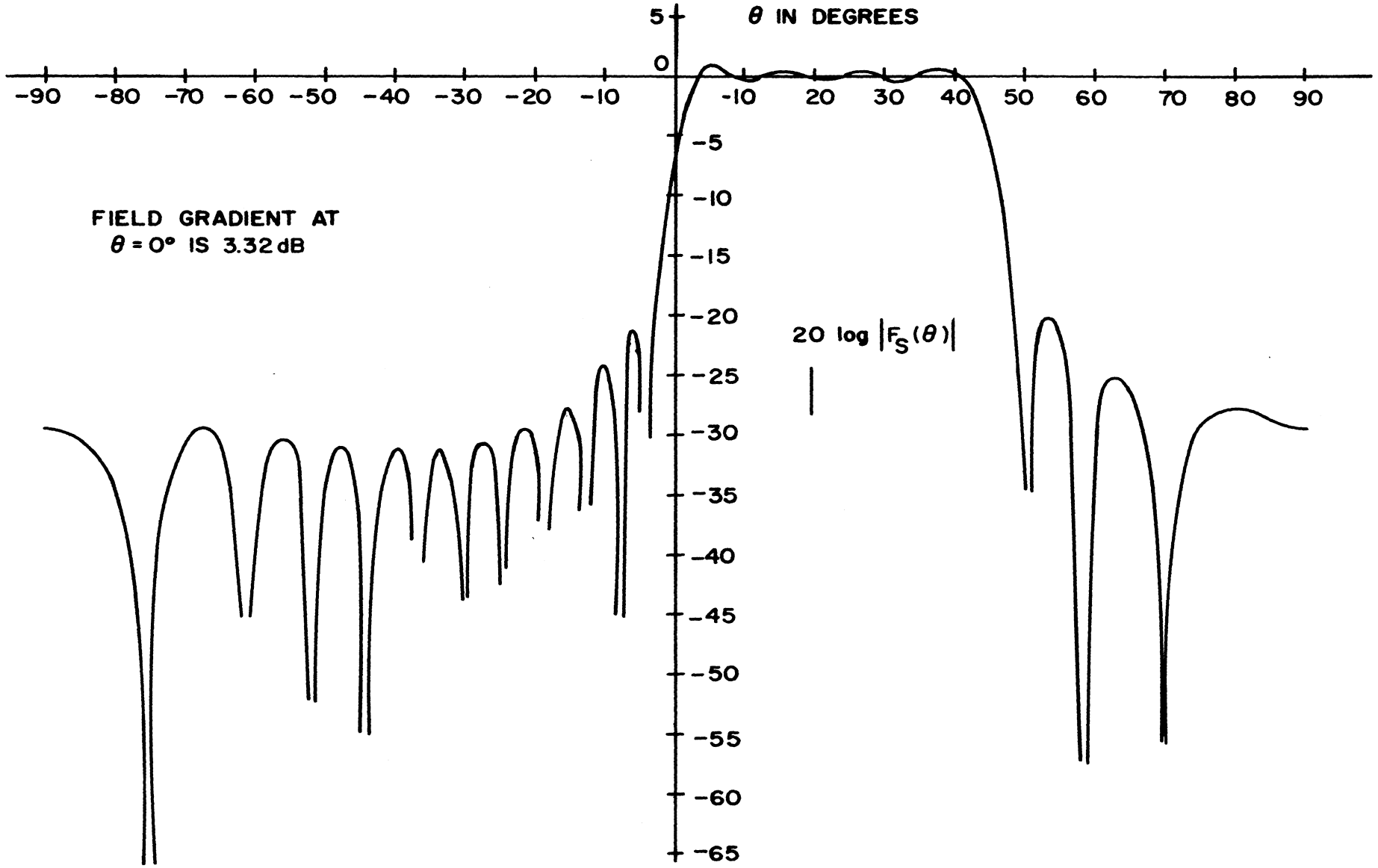

FIG. 10(d): Synthesized pattern for a linear array of (2N+1) elements. $L = 10\lambda$, $N = 10$, $d = \lambda/2$, $\theta_2 = 0$, $\theta_1 = \pi/4$.

3.2 Linear Aperture of Even Number of Elements

Consider a linear aperture of length L aligned along the x-axis which lies in the vertical direction. The aperture consists of an array of 2N isotropic elements, uniformly spaced with interelement spacing d, as shown in Fig. 11. Note that in the

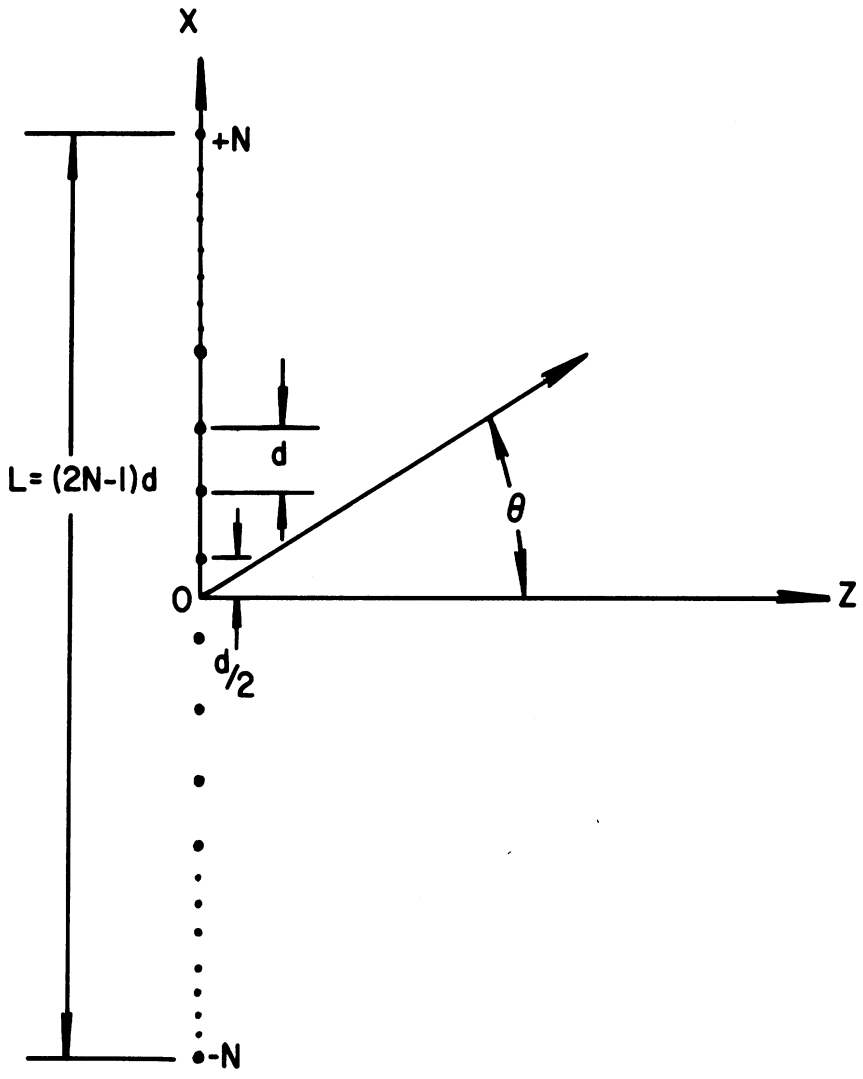

FIG. 11: Linear array of 2N isotropic sources spaced d apart.

present case the total length of the aperture is given by

$$L = (2n - 1)d \tag{26}$$

i.e., for $d = \lambda/2$,

$$L/\lambda = (N - \frac{1}{2}) \ .$$

It is assumed that the interelement spacing $d = \lambda/2$. Following the same procedure as in Section 3.1, it can be shown that the synthesized pattern is given by

$$F_s(\theta) = \sum_{-N}^{N}{}' I_n e^{-i\alpha_n} e^{in\frac{\pi}{2}\sin\theta} \ , \tag{27}$$

where the prime on the summation indicates that the $n = 0$ term is omitted. The array excitation coefficients I_n, α_n are given by

$$I_n = \frac{\sin\left[(2n-1)\frac{\pi}{4}(\sin\theta_1 - \sin\theta_2)\right]}{(2n-1)\frac{\pi}{4}} \ , \tag{28}$$

$$\alpha_n = (2n-1)\frac{\pi}{4}(\sin\theta_1 + \sin\theta_2) \ . \tag{29}$$

For negative values of n, the excitation coefficients in Eq. (27) are obtained from Eqs. (28) and (29) using the relations

$$I_{-n} = I_n \ , \qquad \alpha_{-n} = -\alpha_n \ . \tag{30}$$

Using the above relations the synthesized pattern can be written explicitly as

$$F_s(\theta) = 2\sum_{1}^{N} \frac{\sin\left[(2n-1)\frac{\pi}{4}(\sin\theta_1 - \sin\theta_2)\right]}{(2n-1)\frac{\pi}{4}} \cos\left[(2n-1)\frac{\pi}{2}\left(\sin\theta - \frac{\sin\theta_1 + \sin\theta_2}{2}\right)\right] \tag{31}$$

As before, we study the patterns for $\theta_2 = 0$ for which case Eq. (31) reduces to

$$F_s(\theta) = 2\sum_{1}^{N} \frac{\sin\left[(2n-1)\frac{\pi}{4}\sin\theta_1\right]}{(2n-1)\frac{\pi}{4}} \cos\left[(2n-1)\frac{\pi}{2}\sin\theta - \frac{\sin\theta_1}{2}\right] \tag{32}$$

The pattern slope at θ is obtained by differentiating Eq. (32) with respect to θ and is given by

$$F'_s(\theta) = 2\cos\theta\left\{\frac{\sin(N\pi\sin\theta)}{2\sin\frac{\pi}{2}\sin\theta} - \frac{\sin\left[N\pi(\sin\theta-\sin\theta_1)\right]}{2\sin\left[\frac{\pi}{2}(\sin\theta-\sin\theta_1)\right]}\right\} \quad . \tag{33}$$

The values of $F_s(\theta)$ and $F'_s(\theta)$ at the horizon $\theta = 0^o$ may be obtained from Eqs. (32) and (33) and are given by

$$F_s(0) = \sum_1^N \frac{\sin\left[(2n-1)\frac{\pi}{4}\sin\theta_1\right]}{(2n-1)\frac{\pi}{4}} \tag{34}$$

$$F'_s(0) = 2\left[N - \frac{\sin(N\pi\sin\theta_1)}{2\sin\left(\frac{\pi}{2}\sin\theta_1\right)}\right] \quad . \tag{35}$$

Using Eqs. (34) and (35) and the definition of the field gradient at the horizon discussed earlier, the following relationship is obtained.

$$\alpha_g(0) = 0.1518\,\frac{N - \dfrac{\sin(N\pi\sin\theta_1)}{2\sin\left(\frac{\pi}{2}\sin\theta_1\right)}}{\displaystyle\sum_1^N \frac{\sin\left[(2n-1)\frac{\pi}{2}\sin\theta_1\right]}{(2n-1)\frac{\pi}{2}}} \quad . \tag{36}$$

Table 3 gives the field gradient in $dB/1^o$ at the horizon that can be obtained from a linear array of isotropic elements, spaced $\lambda/2$ apart, and containing 2N elements. The results are shown for two values of the parameter θ_1, $\pi/6$ and $\pi/4$.

Figure 12 shows α_g vs. $N\,(= L/\lambda + 1/2)$ for a linear array of 2N elements designed with $\theta_2 = 0^o$ and $\theta_1 = \pi/6$ and $\pi/4$.

Table 3: Field gradient at the horizon $\alpha_g(0)$ in dB/1° for a linear array of 2N elements. $\theta_2 = 0$, $d = \lambda/2$.

$N = \frac{L}{\lambda} + \frac{1}{2}$	$\alpha_g(0)$ in dB/1° $\theta_1 = \pi/6$	$\theta_1 = \pi/4$
2	0.50	0.73
3	1.10	0.95
4	1.36	1.05
5	1.31	1.69
6	1.70	1.78
7	2.33	2.00
8	2.57	2.63
9	2.52	2.62
10	2.91	2.97

Figures 13a and 13b compare the field gradients of linear antennas containing odd and even numbers of elements for two values of θ_1, $\pi/6$ and $\pi/4$. For a given value of N, the total length of the array of odd number of elements is larger than that of even number of elements by $\lambda/2$. This is why the field gradients for the odd numbered arrays are in general larger than those of the even numbered arrays, as shown in Fig. 13. It is interesting to note in Fig. 13 that for certain values of N, the two arrays arrays possess essentially the same field gradient. The practical implication of this is that for certain values of N, there will be a saving of one element by using an even number of elements to achieve the field gradient.

Figures 14a and 14b show the complete theoretical patterns of a linear array of 8 elements designed with $\theta_1 = \pi/6$ and $\pi/4$ respectively.

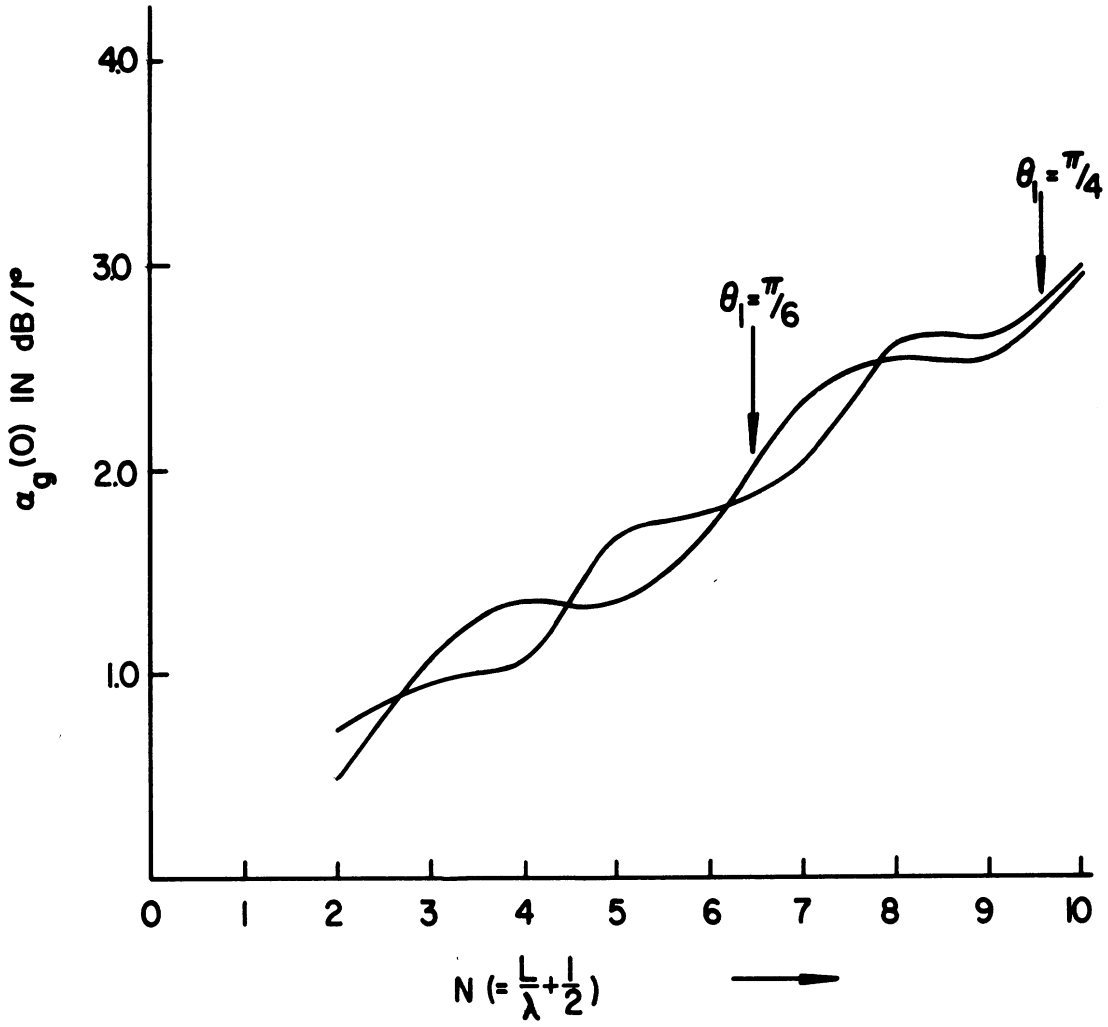

FIG. 12: Field gradient of a linear array of 2N elements as a function of $N (= L/\lambda + 1/2)$ for two values of θ_1.

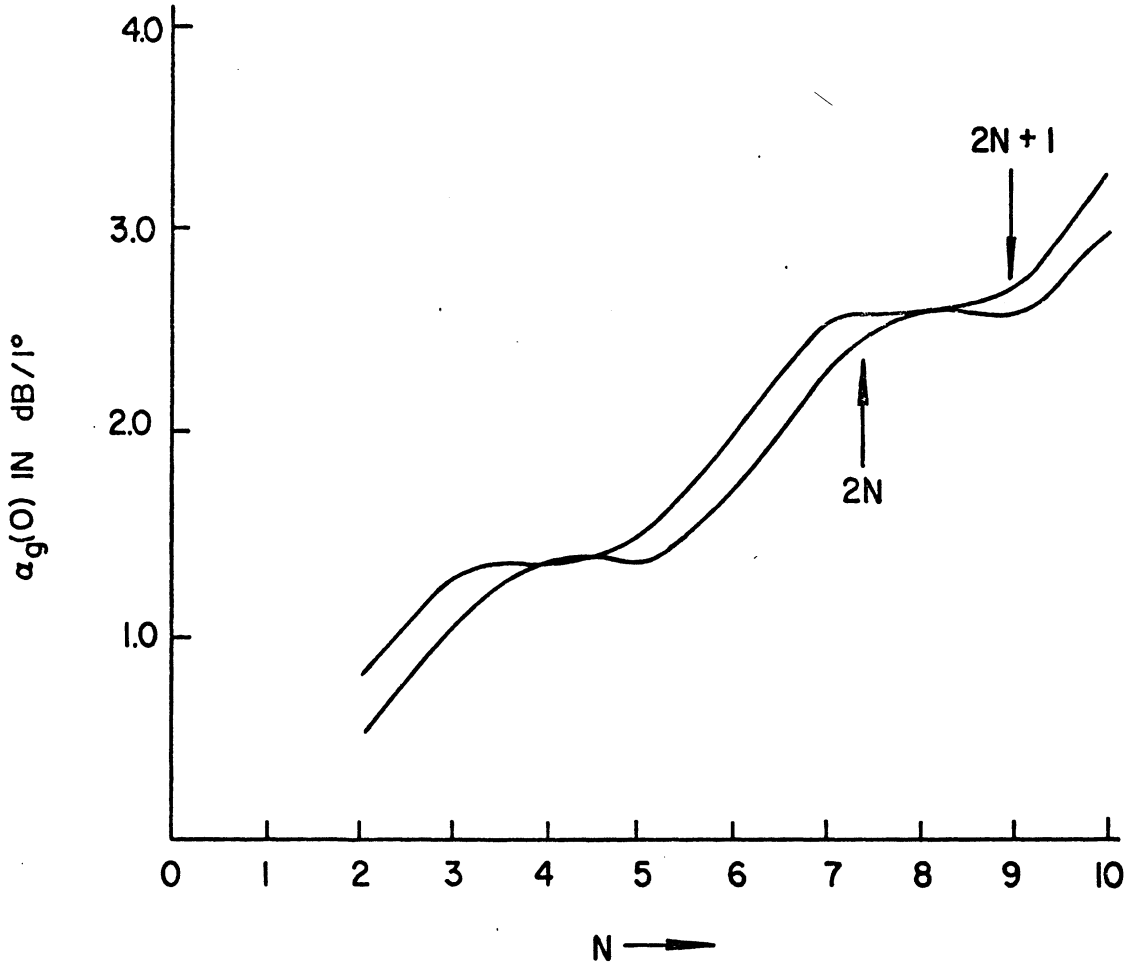

FIG. 13(a): Field gradients of linear arrays of (2N+1) and 2N elements as functions of N. $\theta_1 = \pi/6$.

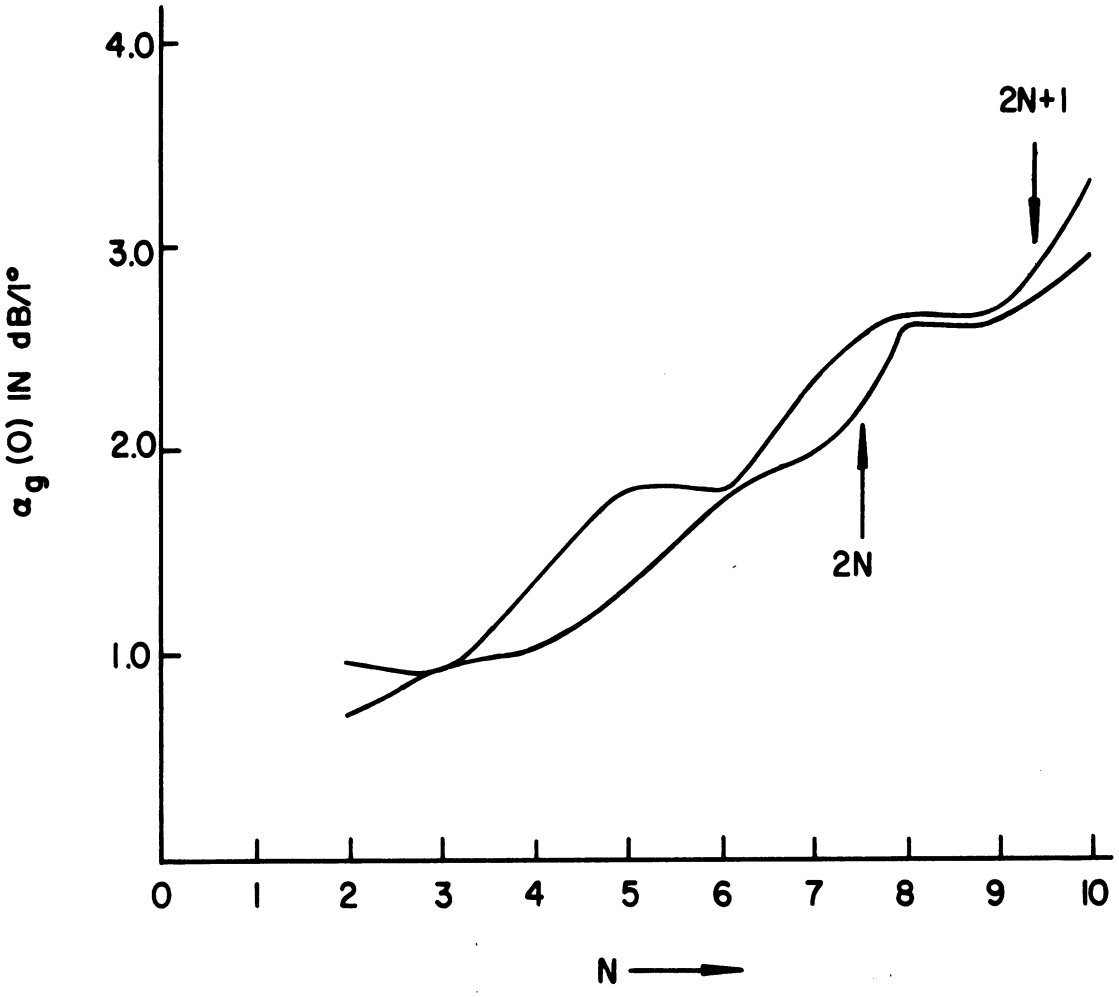

FIG. 13(b): Field gradients of linear arrays of (2N+1) and 2N elements as functions of N. $\theta_1 = \pi/4$.

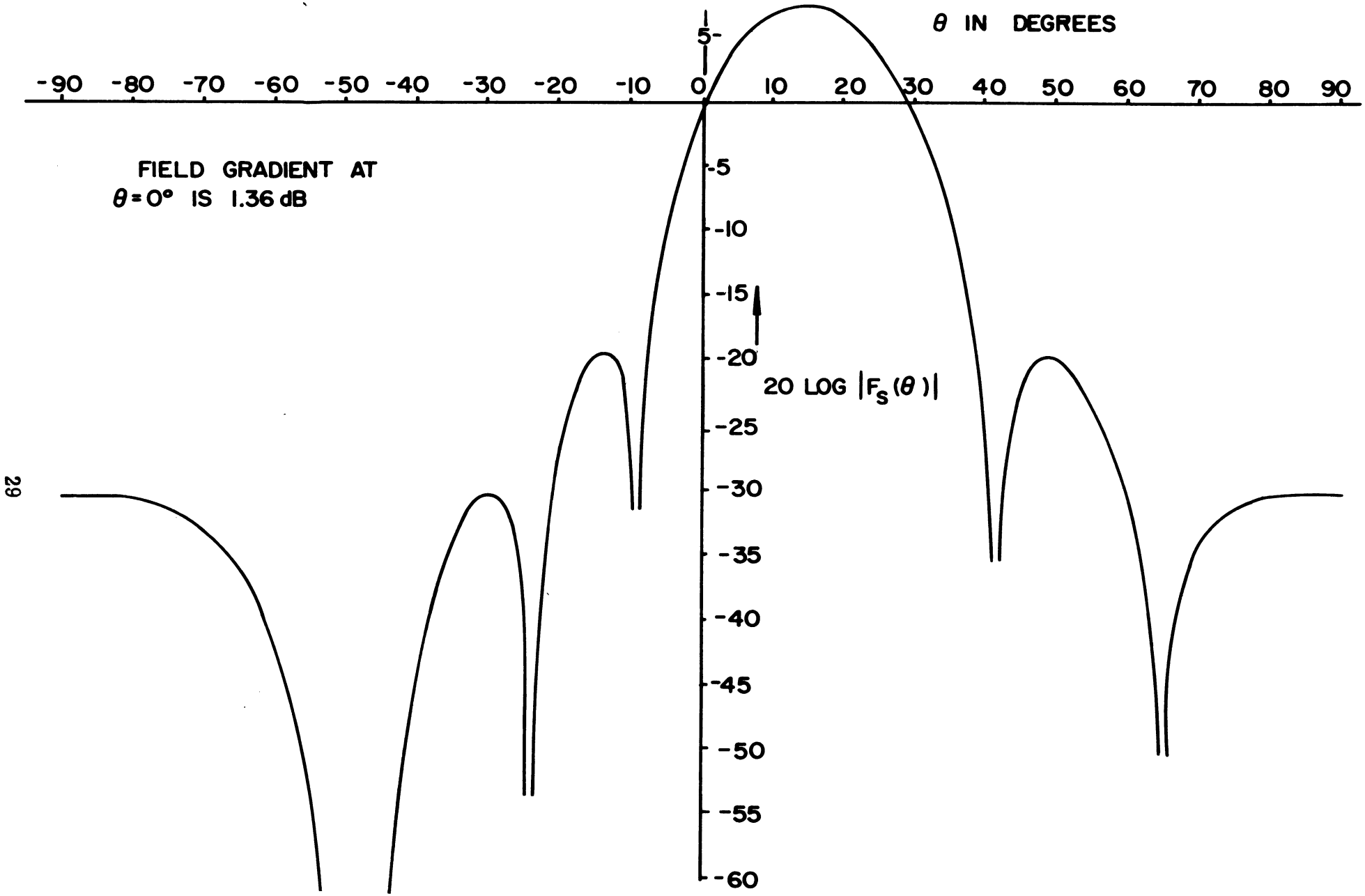

FIG. 14(a): Synthesized pattern for a linear array of 2N elements. N = 4, d = $\lambda/2$, $\theta_2 = 0^{\circ}$, $\theta_1 = \pi/6$.

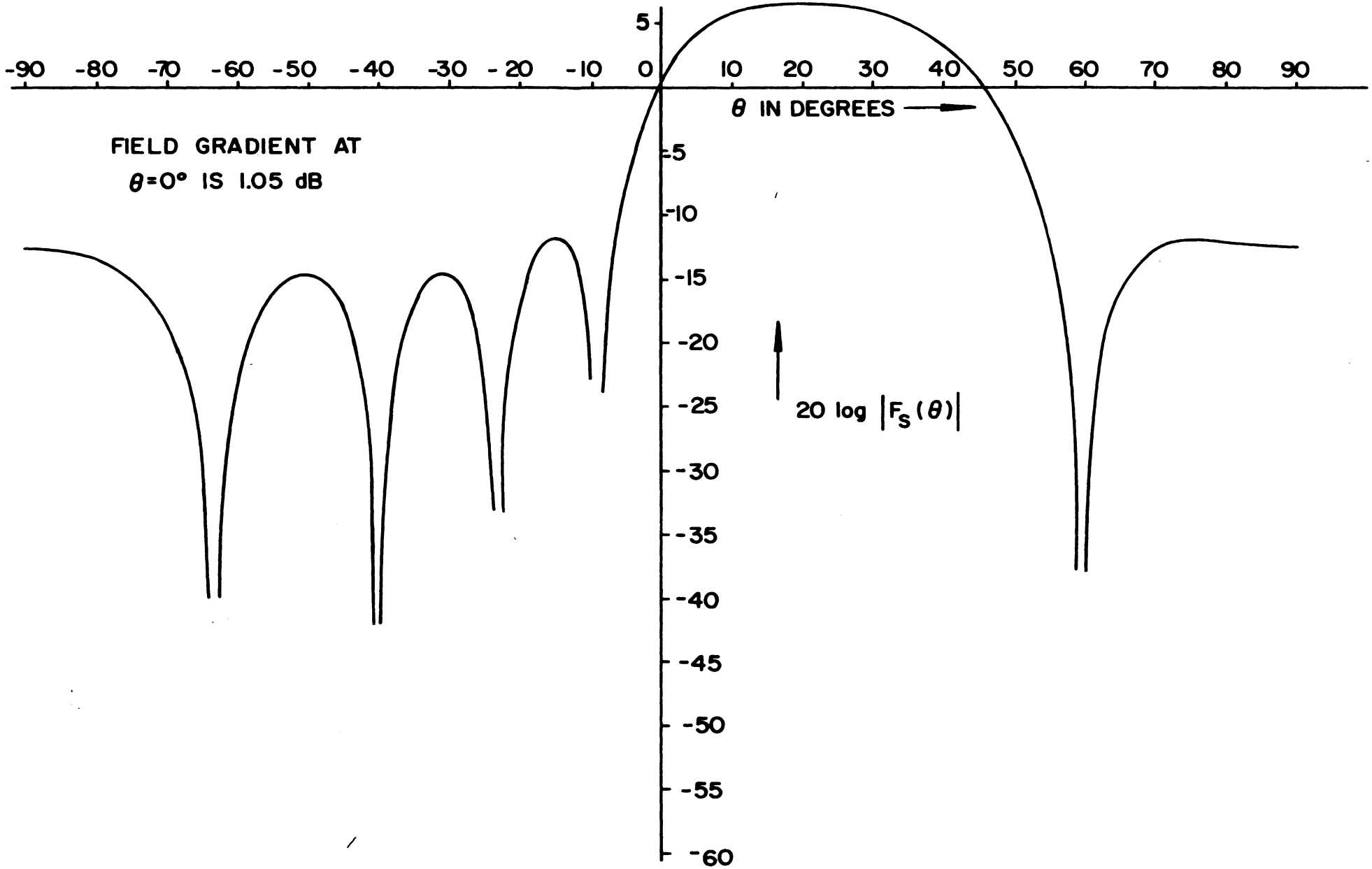

FIG. 14(b): Synthesized pattern for a linear array of 2N elements. N = 4, d = $\lambda/2$, $\theta_2 = 0^o$, $\theta_1 = \pi/4$.

4. DISCUSSION

Fourier synthesis of a sector beam pattern by a linear array of discrete isotropic elements has been discussed. The results have been applied to study the characteristics of the free space vertical plane patterns of the exiting and improved ATCRBS antennas, believed to be designed by Fourier techniques. It is found that the field gradient of such an antenna depends mainly on the overall length of the aperture, i.e., on the number of elements used. The field gradient for a given aperture length may be estimated roughly by using the continuous aperture theory. For better accuracy the discrete elements theory should be used. The expressions derived for the field gradients are found to be fairly accurate.

In the present report we have considered only the method based on Fourier techniques which approximate the desired pattern in the least mean square sense. It should be noted that such a solution does not provide an answer to the question whether the field gradient obtained for a given aperture length is largest. In this sense the present design is not optimum. It is desirable that the problem should be further investigated in the light of the following: is it possible to obtain larger field gradients for a given aperture length if a different error criterion is used to synthesize the pattern, e.g., using the minimax criterion?

5. REFERENCES

[1] J. Zatkalik, D.L. Sengupta and C.T. Tai, "Sidelobe Suppression Mode Performance of ATCRBS with Various Antennas", Report No. FAA-RD-75-31, U.S. Department of Transportation, Federal Aviation Administration, Systems Research and Development Service, Washington, D.C., February 1975.

[2] D.L. Sengupta, J. Zatkalik and C.T. Tai, "Improved Sidelobe Suppression Mode Performance of ATCRBS with Various Antennas", Report No. FAA-RD-75-32, U.S. Department of Transportation, Federal Aviation Administration, Systems Research and Development Service, Washington, D.C., February 1975.

[3] B.M. Poteat, et al., "ATCRBS Antenna Modification Kit: Phase I", Westinghouse Defense and Electronic System Center, Systems Development Division, Baltimore, Maryland, July 25, 1973.

[4] P. Richardson, et al., "Air Traffic Control Radar Beacon System (ATCRBS): Phase I Final Engineering Report", Texas Instruments, Incorporated, Dallas, Texas, October 1973.

[5] V. Mazzola, et al., "ATCRBS Antenna Modification Kit, Phase I", Engineering Report No. 10991, Hazeltine Corporation, New York, 1973.

[6] R.E. Collin and F.J. Zucker, Antenna Theory, Part I, Chapters 3 and 7, McGraw-Hill Book Co., New York, 1973.

APPENDIX A
REPORT OF INVENTIONS

A diligent review of the work performed under this contract has revealed no new innovation, discovery, improvement or invention.